

Phase transitions of the ferroelectric $\text{Na}_{0.5}\text{Bi}_{0.5}\text{TiO}_3$ by dielectric and internal friction measurements

Venkata Ramana Mudinepalli^{1*}, N. Ramamanohar Reddy², Wen-Chin Lin¹, K.V. Siva Kumar³, B.S. Murty⁴

¹Department of Physics, National Taiwan Normal University, Taipei, 11677, Taiwan

²Department of Materials Science and Nanotechnology, Yogi Vemana University, Kadapa, 516 227, India

³Ceramic Composite Materials Laboratory, Department of Physics, Sri Krishnadevaraya University, Anantapur 515003, India

⁴Nanotechnology Laboratory, Department of Metallurgical and Materials Engineering, Indian Institute of Technology-Madras, Chennai, 600 036, India

*Corresponding author. Tel: (+886) 974181313; E-mail: materialphysics.ramana@gmail.com

Received: 28 August 2014, Revised: 16 October 2014 and Accepted: 15 November 2014

ABSTRACT

This work focuses on the high temperature dielectric and mechanical spectroscopic properties of lead free relaxor Sodium Bismuth Titanate (NBT) ceramics, fabricated by conventional ceramic double sintering method. Systematic measurements of dielectric and mechanical properties have been performed as a function of temperature. A sequence of phase transitions has been studied by both dielectric and anelastic measurements. Three internal friction peaks were observed near 350, 200 and 120 °C. The 350 °C-peak corresponds to a transition associated with the tetragonal ($P4bm$) to rhombohedral ($R3c$) phase, and the 200 °C-peak is related to the ferroelectric to antiferroelectric phase transition. The 120 °C-peak could be ascribed to the interaction between the domain walls and the diffusion of oxygen vacancies in the domains. Copyright © 2015 VBRI Press.

Keywords: Internal friction; ferroelectric; elastic modulus; dielectric; phase transition; Curie transition temperature.



Venkata Ramana Mudinepalli is working as a Post Doctoral Research Associative at Department of Physics, National Taiwan Normal University, Taipei, Taiwan. He obtained his PhD., in 2008 from Sri Krishnadevaraya University, Anantapur, India. He has been recipient of several fellowships like Senior Research Fellowship from DRDO, India, Research Associative from IIT Madras, Shenzhen Post Doctoral Research Fellowships. He has published more than 30 research papers in reputed International

journals. His current research is focused on magnetic nano thin films for gas sensors.

Introduction

Lead-based ceramics like PZT, PMN-PT and PZN-PT are extensively used as the materials for sensors, actuator and transducers in the electronic industry because of their high piezoelectric coefficients [1]. However, the toxicity of lead has raised concerns about lead-based piezoelectric materials. Therefore, lead-free functional materials are highly desirable for environment-friendly applications. In this context, sodium bismuth titanate $\text{Na}_{0.5}\text{Bi}_{0.5}\text{TiO}_3$ (NBT) was found to be ferroelectric (rhombohedral symmetry) at

room temperature with its Curie temperature near 320°C. NBT has been considered as an excellent candidate for lead-free piezoelectric ceramics due to its large remnant polarization ($38 \mu\text{C}/\text{cm}^2$) and coercive field (73 kV/cm) at room temperature and a high conductivity. NBT undergoes two phase transitions on heating: (i) rhombohedral to tetragonal phase at about 200°C, (ii) tetragonal to paraelectric cubic phase at about 520°C (T_c) [2]. Also, its permittivity displays a very interesting anomaly at about 200°C where the depolarization occurs and the dielectric anomaly exhibits small relaxor characteristics [3]. Some researchers suggest that the NBT undergoes a transition from the ferroelectric to antiferroelectric phase at the depolarization temperature, T_d [4, 5]. However, it has not been confirmed that an antiferroelectric phase exists in NBT ceramics in the temperature range of T_d - T_c [6]. The tetragonal phase seems to be ferroelastic without any dielectric anomaly at the transition to the cubic phase. However, the question of whether this phase is polar is still open. Much of the unexplained behavior has been found in the range between the ferroelastic and ferroelectric phases [5]. Some dielectric measurements indicate that an antiferroelectric phase exists between the tetragonal ferroelastic and rhombohedral ferroelectric phases [7].

However, X-ray and neutron-scattering studies have not provided any evidence in support of this view [8, 9].

Internal friction is very sensitive and effective in detecting atomic rearrangements and kinetics of atomic movements involved in microstructural evaluations. Internal friction is a controversial problem to identify the phase transitions in the ceramic materials. Mechanical spectroscopy is a technique which operates in the anelastic range, applying an oscillating stress to a specimen and then inducing the structural defects motion (point defects, dislocations, etc.). The mobility of these defects, which is intrinsically related to the mechanical properties of material, can be investigated by this technique. Furthermore, mechanical spectroscopy has also the advantage of being a non-destructive technique, and therefore very useful when not much material is available and many experiments have to be performed under different conditions. As reported by many workers [10, 11], among the verity of experimental methods for the measurement of physical properties, the internal friction method has special scientific importance because of its high sensitivity to structural rearrangements, especially to the point defects [12], phase transitions [13] and domain walls [14, 15]. Our previous work on the PZT shows two internal friction peaks and the results are similar to that reported by Bourim [15]. Recently Cordero et al. [16] have been studied the phase transitions and phase diagram of ferroelectric ceramics of $(\text{Na}_{0.5}\text{Bi}_{0.5})_{1-x}\text{Ba}_x\text{TiO}_3$ with $x=0$ and $x=2, 3, 4, 5, 6, 8$ mol % were prepared following the mixed-oxide method and measured by anelastic and dielectric properties. Zhang et al. [16] have studied the dynamic mechanical properties of $(\text{Bi}_{0.5}\text{Na}_{0.5})_{1-x}\text{Ba}_x\text{TiO}_3$ ($x=0.05, 0.06, 0.07, 0.08, 0.10, 0.15, 0.20, 0.25, 0.30$) ceramics synthesized by modified citrate method. Uddin et al. [18] have also been studied on sol-gel prepared single phase $(1-x)\text{Bi}_{1/2}\text{Na}_{1/2}\text{TiO}_3 - x\text{BaTiO}_3$ ($0 \leq x \leq 0.06$) ceramics by low frequency dynamic mechanical method to identify the phase transitions.

The internal friction may inhibit the movement of domain walls and interaction of point defects with the domain walls and other imperfections. The elastic constants should provide clear information on the occurrence of phase transformations of cubic, tetragonal, and rhombohedral phases which are of ferroelectric in nature. But only few studies of the acoustic properties of NBT exist. In the present paper, we show the experimental results of high temperature and high frequency internal friction (Q^{-1}) and longitudinal modulus (L) results on the pure $\text{Na}_{0.5}\text{Bi}_{0.5}\text{TiO}_3$. Also compare this properties with dielectric and ferroelectric properties to confirm exist phases in the relaxor lead free NBT ceramic for the first time.

Experimental

Materials

The NBT ceramic was synthesized via conventional solid state reaction route. The starting powders of Na_2CO_3 , Bi_2O_3 and TiO_2 (99% of purity, German made Merck) were ball milled in Fritsch P5 high energy planetary ball mill in an ethyl alcohol medium for 20 h with a ball to powder weight ratio of 10:1 at a speed of 300 rpm for 40 h. The slurry was dried and the dried powders were loosely packed in the

form of cakes. These cakes were calcined in closed alumina crucibles at 700 °C for 4 h. After calcinations, these cakes were crushed and powdered. These powders were ball-milled once again under the same conditions in ethyl alcohol medium for 8 more hours to obtain a fine particle size. The milled powders were compacted uniaxially at 100 MPa to make a green compact with the dimensions of 3.5 mm × 3.5 mm × 20.5 mm bars for measurements of longitudinal modulus and internal friction. For dielectric and ferroelectric properties, pellets of 10 mm in diameter and 2 mm in thickness were prepared using a uniaxial hydraulic press.

Structural analysis

X-ray powder diffraction patterns were recorded on a Philips, PW-1710 diffractometer using $\text{CuK}\alpha$ radiation. Transmission electron microscopy (TEM) was performed using a Philips CM 20 microscope for the sintered sample. The dielectric properties were measured with the use of a HIOKI LCR Hi-tester. The polarization and electric field (P-E) hysteresis loops were obtained by a Radiant Technologies ferroelectric test system with virtual ground mode at 1 kHz. The high frequency (104 kHz) internal friction (Q^{-1}) and longitudinal modulus (L) measurements were measured on composite oscillator, as a function of temperature at a heating rate of 5°C/min and Q^{-1} and L data obtained in the present work are accurate to ± 5 and ± 2 , respectively. From the resonant frequency (f_s) of the composite system and the logarithmic decrement (δ), the Q^{-1} and L have been evaluated using the standard relations as detailed in the literature [19, 20]. The x-cut quartz transducer used in the present investigation has a length of 2.653×10^{-2} m, width of 3.32×10^{-3} m, natural frequency 104.387 kHz and a mass of 1.0316×10^{-3} kg. The electrode faces were painted with conducting silver paint (Du Pont). The composite oscillator was formed by cementing the quartz transducer to the specimen of identical cross-section. The adhesive used in this work was a paste containing one part by weight of calcium carbonate and five parts by weight of sodium metasilicate in a small quantity of distilled water. The composite system works satisfactorily after it has been kept for 24 h at room temperature. In order to study the effect of temperature on internal friction and longitudinal modulus of the NBT specimens, the composite resonator system with the sample holder was placed at the center of a tubular electric furnace. All the internal friction measurements were performed with strain amplitude of 10^{-6} , after the specimen had attained thermal equilibrium.

Results and discussion

The measured density of the prepared ceramic was 5.73 g/cm³, being about 96% of the theoretical value (5.97 g/cm³). The XRD pattern of the ceramic (Fig. 1) shows a single perovskite phase with a rhombohedral ($R3c$) symmetry. A superlattice peak at 38.38° can also be observed, which characterizes the space group $R3c$. A similar type of behavior was also observed in NBT earlier with an XRD peak at 38.4° [21]. The inset in the figure shows the TEM bright field image, which indicates that the grain size of NBT is around 100 nm even after sintering.

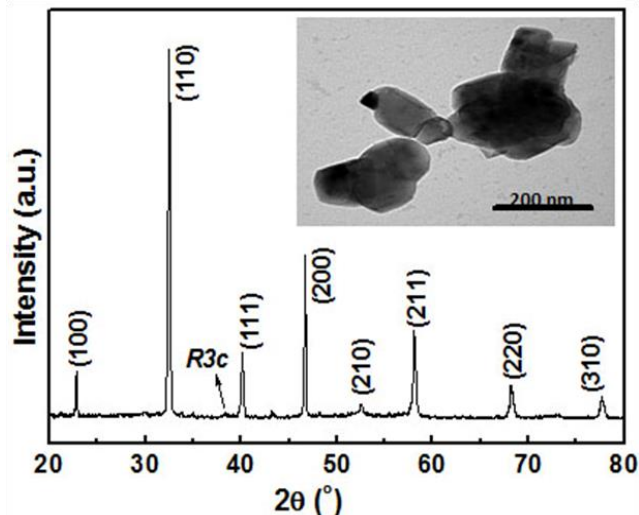


Fig. 1. XRD pattern and TEM bright field image (inset) of $\text{Na}_{0.5}\text{Bi}_{0.5}\text{TiO}_3$ at room temperature.

Dielectric properties

The temperature dependences of dielectric constant and the loss tangent $\tan\delta$ at three different frequencies are shown in Fig. 2. The diffusional phase transformation is observed with a broad dielectric maximum at around 350°C (T_c) corresponding to a transition from an anti-ferroelectric to a paraelectric phase, near and beyond which the dielectric constant is frequency independent. The maximum dielectric constant decreases with increasing frequency. The so-called depolarization temperature (T_d) inherent to NBT is located at around 200°C , (T_d , corresponding to a change from a ferroelectric phase to an anti-ferroelectric phase). The T_d shows the relaxor behavior and is frequency dependent, which shifts to higher temperatures with increasing frequency. At T_d , the specimen is basically depolarized and loses piezoelectric activity. When the frequency increases, the permittivity at T_d decreases and its maximum is shifted towards higher temperatures in a similar way to that observed in relaxor materials [4]. It is seen from Fig. 2(a) that the ceramic possesses dielectric constants of approximately 798 and 3324 at room temperature and T_c , respectively, at a frequency of 50 kHz. Also, it is possible to obtain the T_d from the temperature dependence of $\tan\delta$, which is determined by the inflexion of the curve at around 200°C , as shown in the inset of Fig. 2(b). Thus, it is concluded that the dispersion in dielectric constant and loss factor is similar to that of the relaxor below T_c [1], indicating polar heterogeneities with low frequency fluctuations.

Ferroelectric properties

Fig. 3 shows the polarization (P-E) hysteresis loops for the prepared NBT at various temperatures. At room temperature, the P-E loop saturated for $\leq 40\text{ kV/cm}$ exhibits a typical shape for ferroelectrics. The saturation polarization (P_s), remnant polarization (P_r) and coercive field (E_c) are $44.45\mu\text{C/cm}^2$, $38.8\mu\text{C/cm}^2$, and 19.16 kV/cm , respectively. The values of P_s , P_r , and E_c reduce slightly with increasing temperature in the range 30°C - 200°C . At 120°C , the material still shows the ferroelectric behavior.

However, when the temperature reaches to 150°C which is close to T_d , the P-E loop starts to deform, and gradually becomes the double hysteresis loop which is attributable to an antiferroelectric phase. As a consequence, the hysteresis loop becomes “pinched” and almost a double-like hysteresis loop, which could indicate the coexistence of ferroelectric (FE) and nonpolar phases. With further increasing of temperature to T_d ($\sim 200^\circ\text{C}$), the nonpolar phase becomes dominant, as indicated by the P-E loop. These results are in good agreement with previous reports [4, 21-26]. The temperature dependence of P_s and P_r is summarized in Fig. 3(f).

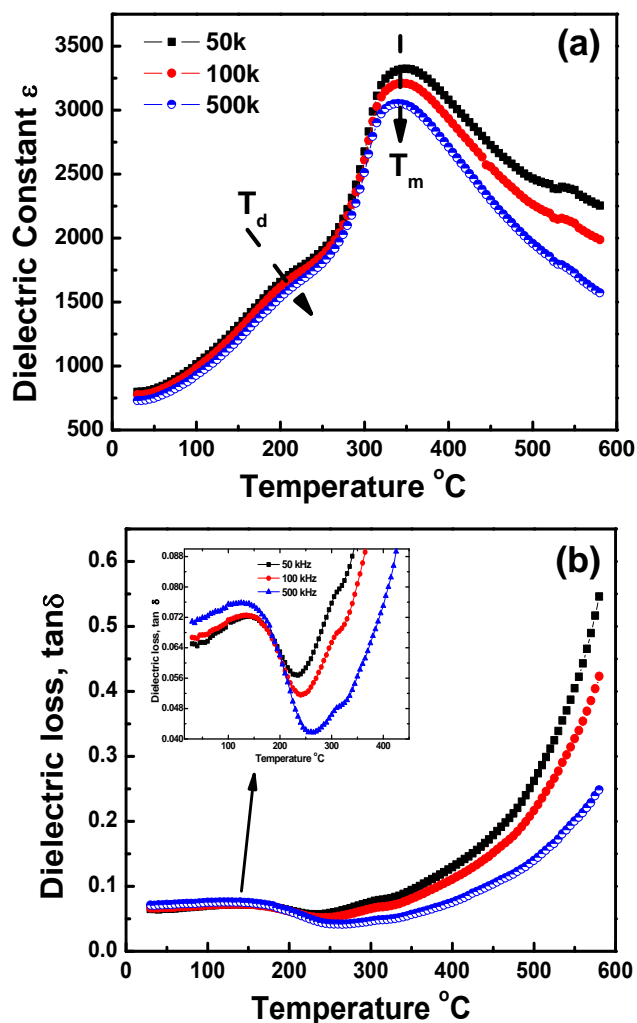


Fig. 2. Variation of (a) dielectric constant and (b) dielectric loss of $\text{Na}_{0.5}\text{Bi}_{0.5}\text{TiO}_3$ with temperature at different frequencies. (Inset: Variation of dielectric loss of NBT at low temperatures).

As seen, the most notable change is a sharp drop in P_r from $38\mu\text{C/cm}^2$ at 30°C to $9\mu\text{C/cm}^2$ at 120°C , which then asymptotically converges to zero on heating to T_d . P_s also decreases from 44 to $16\mu\text{C/cm}^2$ with increasing temperature between 30°C and 200°C . The measured spontaneous and remnant polarization are in good agreement with those reported for ferroelectric $0.885(\text{Bi}_{1/2}\text{Na}_{1/2})\text{TiO}_3$ – $0.05(\text{Bi}_{1/2}\text{K}_{1/2})\text{TiO}_3$ – $0.015(\text{Bi}_{1/2}\text{Li}_{1/2})\text{TiO}_3$ – 0.05BaTiO_3 ceramics by Tai et al. [27].

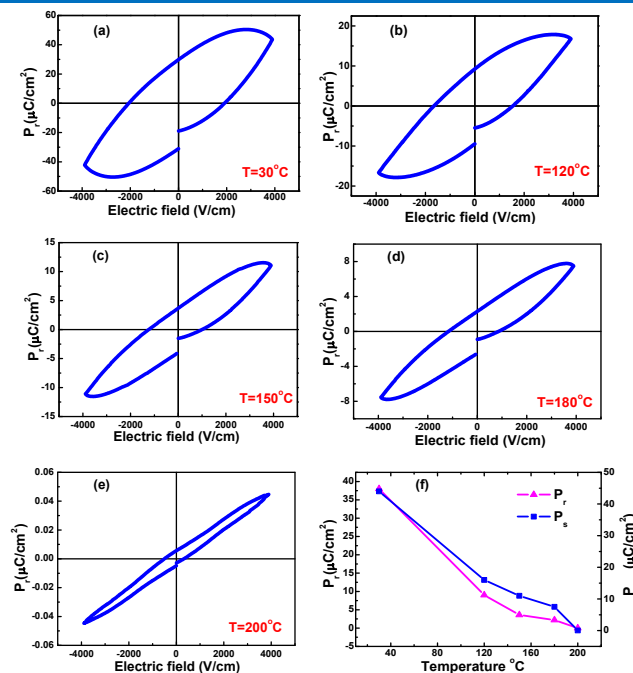


Fig. 3. (a) to (e) P-E hysteresis loops of $\text{Na}_{0.5}\text{Bi}_{0.5}\text{TiO}_3$ at different temperatures. (f) Temperature dependence of the (P_r) and (P_s).

Longitudinal modulus and internal friction properties

The great interest in the method based on the measurement of internal friction in the investigations of ceramic materials is caused by the fact that, the information about the behavior of a material on atomic level can be obtained by observing macroscopic vibrations of the material. This method is characterized by its high sensitivity to changes in the concentration of point defects, to the interaction between the defects, and to changes in the structure of materials [28]. In the ferroelectrics, the domain boundary movement is limited by the different lattice imperfections such as interstitials, vacancies and dislocations. The point defects, for example, may play the role of stoppers for domain boundaries and they can result in the hysteresis losses due to unpinning at domain boundaries. Therefore the interaction of point defects with the domain boundaries, which leads to the internal friction, is of great interest.

The temperature dependence of internal friction and longitudinal modulus for the prepared NBT ceramic sample has been measured at a frequency of 104 kHz on heating, as shown in Fig. 4. Clearly, the longitudinal modulus decreases overall with temperature, and shows three anomalies during heating at 120°C, 200°C and 350°C. Three internal friction peaks emerge at 120 (P3), 200 (P2) and 350°C (P1) which are associated with the longitudinal anomalies. The crystal structure of NBT transforms on cooling from (i) the P1 peak corresponding to a transition of the tetragonal ($P4bm$) to rhombohedral ($R3c$) at around 350°C [5, 21], to (ii) the P2 peak relating to the ferroelectric to antiferroelectric phase transition at around 200°C [5, 7, 29, 30]. These results are consistent with the experimental results on NBT single crystals produced by Czocharlski method by use of pulse echo method [29]. The two internal friction peaks P1 (350°C) and P2 (200°C) are associated with dielectric properties, but the peak position shows the relaxor behavior with frequency. It is interesting to note the 120°C-internal friction peak may not be

recognized in the temperature dependence of dielectric constant. This phenomenon has the characteristic of a static hysteresis type.

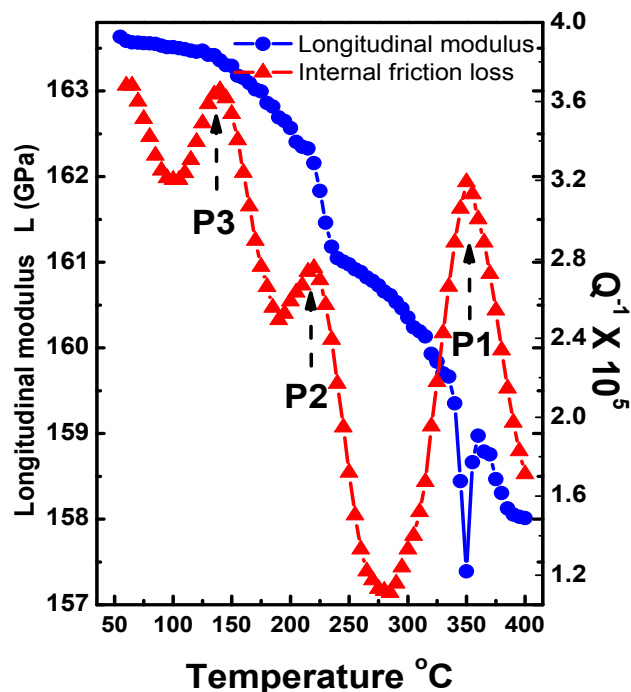


Fig. 4. Temperature dependence of longitudinal modulus and internal friction of $\text{Na}_{0.5}\text{Bi}_{0.5}\text{TiO}_3$.

To explain this, we suppose that the P3 peak is due to the formation of anisotropic anelastic dipoles between oxygen vacancies and cation ions. These dipoles present a low symmetry compared to the whole crystal lattice. The re-orientation of the dipole can take place by the jump of the vacancies around the cation ions under the applied torsion stress, resulting in mechanical relaxation. The P3 peak may be ferroelectric (rhombohedral) to antiferroelectric (tetragonal) phase transition. According to Wang's theory [31], in ferroelectric/ferroelastic phase, the density of domain walls increases with increasing temperature and is approximately proportional to $1/(T_c - T)$ when temperature T was near the phase transition (ferroelectric) temperature (T_c), leading to an increase in Q^{-1} . On other hand, the distance between domain walls decreases due to the increase in their density and results in an increase in the mobility of domain walls because of their interactions, thus leading to a decrease in Q^{-1} . The compromise of the above two factors brings about the internal friction peak. However, P-E hysteresis loop measurements reveal that the NBT ceramic still shows the ferroelectric behavior at 120 °C.

The internal friction peak due to oxygen vacancies in the high temperature range has been found in some perovskite -structure ceramics. Postnikov et al. [32] have measured this type of internal friction peak in PZT above room temperature. They consider energy losses due to vibration damping of 90° domain walls caused by their interaction with oxygen vacancies. Nevertheless, without domain walls, the migration of oxygen vacancies alone can also induce an internal friction peak in YBCO ceramics [33], and jumps of oxygen vacancies between two unequal

lattice sites O_A (1/2,0,0) and O_B (0,1/2,0) may induce a high internal friction peak.

From the above results, it can be found that the internal friction peak of the NBT ceramic at 120°C can be induced by several mechanisms because NBT ceramics have domain walls (like PZT) and unequal oxygen positions (like YBCO) at around 120°C. However, all of the possible relaxation processes could be related to the migration of oxygen vacancies, which is well consistent with previous results [34]. In other words, it can be considered that the internal friction peak is caused by oxygen vacancies, but when the density of oxygen vacancies is too high, the internal friction peak will disappear. This phenomenon may be ascribed to the disappearance of the ferroelectric property of the sample due to out-diffusion of a large amount of oxygen. Normally, the interaction between point defects and other imperfections, such as dislocations and domain walls, can induce internal friction. In our sample, the point defects are oxygen vacancies. Since the ferroelectricity is related to the crystal imperfection, it is assumed that the internal friction peak is due to the interaction between oxygen vacancies and domain walls. On the other hand, it was found that the peak height increased with the vibration amplitude, which was one of the characteristics of the internal friction peak due to the pinning of point defects [35].

The relatively weak domain wall pinning in NBTs may result from other factors besides the magnitude of ferroelectric polarization. For instance, Pb loss in PZTs leads to the formation of compensating point defects [36]. In SBTs, the absence of a volatile cation on the A-site results in a smaller oxygen vacancy concentration in the perovskite sublattice. This effect may also contribute to the weaker domain wall pinning in NBTs. The volatility of Bi_2O_3 may result in oxygen vacancies in the Bi-containing layers, and their role in stabilizing charge trapping at domain boundaries is likely to be less important than oxygen vacancies in the perovskite sublattice. This is because the ferroelectric polarization in NBTs and similar materials is due mostly to ionic displacements within the perovskite sublattice [37].

Conclusion

In summary, the polycrystalline NBT ferroelectric ceramic has been studied by internal friction and dielectric measurements. The dielectric study indicates that the phase transition of the NBT is of diffusional type and well above the room temperature. Three internal friction sharp peaks are detected. The P1 (~350°C) peak is associated with the tetragonal ($P4bm$) to rhombohedral ($R3c$) phase transition, the P2 (~200°C) peak is related to the ferroelectric to antiferroelectric phase transition. Another low temperature peak P3 (~120°C) may be related to a complex mechanism including the viscous motion of domain walls and the interaction between point defects and domain walls. Since the internal friction is sensitive to oxygen vacancies and domain walls, the internal friction study for ferroelectric materials may provide helpful information to understand the structure and dynamical processes of the defects, and their influence on the properties of materials.

Reference

1. L.E. Cross, *Ferroelectrics* **1994**, *151*, 305.
DOI: [10.1080/00150199408244755](https://doi.org/10.1080/00150199408244755)
2. G.A. Smolenskii, V.A. Isupov, A.L. Agranovskaya, N.N. Krainik, *Sov. Phys. Solid. State* **1961**, *2*, 2651.
3. S.D. Said, J.P. Mercurio, *J. Eur. Ceram. Soc.* **2001**, *21*, 1333.
DOI: [10.1016/S0955-2219\(01\)00012-7](https://doi.org/10.1016/S0955-2219(01)00012-7)
4. I.G. Siny, C.-S. Tu, V.H. Schmidt, *Phys. Rev. B* **1995**, *51*, 5659.
DOI: [10.1103/PhysRevB.51.5659](https://doi.org/10.1103/PhysRevB.51.5659)
5. C.-S. Tu, I.G. Siny, V.H. Schmidt, *Phys. Rev. B* **1994**, *49*, 11550.
DOI: [10.1103/PhysRevB.49.11550](https://doi.org/10.1103/PhysRevB.49.11550)
6. J. Suchanicz, *Ferroelectrics* **1998**, *209*, 561.
DOI: [10.1080/00150199808018070](https://doi.org/10.1080/00150199808018070)
7. K. Sakata, Y. Masuda, *Ferroelectrics*, **1974**, *7*, 347.
DOI: [10.1080/00150197408238042](https://doi.org/10.1080/00150197408238042)
8. J.A. Zvirgzds, P.P. Kapostins, J.V. Zvirgzde, T.V. Kruzina, *Ferroelectrics*, **1982**, *40*, 75.
DOI: [10.1080/00150198208210600](https://doi.org/10.1080/00150198208210600)
9. S.V. Vakhrushev, B.E. Kvyatkovsky, R.S. Malysheva, N.M. Okuneva, E.L. Plachenova, P.P. Syrnikov, *Sov. Phys. Crystallogr* **1989**, *34*, 89.
10. Y.R. Dai, P. Bao, H.M. Shen, D. Su, J.S. Zhu, Y.N. Wang, *Appl. Phys. Lett.* **2003**, *82*, 109.
DOI: [10.1063/1.1534610](https://doi.org/10.1063/1.1534610)
11. E.M. Bourim, H. Tanaka, *J. Appl. Phys.* **2002**, *91*, 6662.
DOI: [10.1063/1.1469201](https://doi.org/10.1063/1.1469201)
12. F. Yan, Y.N. Wang, J.S. Liu, Z.G. Zhang, X.B. Chen, *Appl. Phys. Lett.* **1999**, *74*, 2794.
DOI: [10.1063/1.124016](https://doi.org/10.1063/1.124016)
13. B.L. Cheng, M. Gabbay, W. Duffy, G. Fantozzi, *J. Mater. Sci.* **1996**, *31*, 4951.
DOI: [10.1007/BF00355886](https://doi.org/10.1007/BF00355886)
14. S.A. Gridnev, V.S. Postnikov, *Ferroelectrics* **1980**, *29*, 157.
DOI: [10.1080/00150198008008471](https://doi.org/10.1080/00150198008008471)
15. E.M. Bourim, H. Tanaka, M. Gabbay, G. Fantozzi, *Jap. J. Appl. Phys.* **2000**, *39*, 5542.
DOI: [iopscience.iop.org/1347-4065/39/9S/5542](https://doi.org/10.1080/00150198008008471)
16. F. Cordero, F. Craciun, F. Trequatrini, E. Mercadelli, C. Galassi, *Phys. Rev. B* **2010**, *81*, 144124.
DOI: [10.1103/PhysRevB.81.144124](https://doi.org/10.1103/PhysRevB.81.144124)
17. Xiu-Cheng Zheng, Guang-Ping Zheng, Zheng Lin, Zhi-Yuan Jiang, *Ceram. Inter.* **2013**, *39*, 1233.
DOI: [10.1103/PhysRevB.81.144124](https://doi.org/10.1103/PhysRevB.81.144124)
18. Sarir Uddin, Guang-Ping Zheng, Yaseen Iqbal, Rick Uvic, Ngai Yui Chan, Helen Lai Wa Chan, *Mater. Res. Exp.* **2014**, *1*, 046102.
DOI: [10.1088/2053-1591/1/4/046102](https://doi.org/10.1088/2053-1591/1/4/046102)
19. M. Venkata Ramana, G. Sreenivasulu, N. Ramamanohar Reddy, K.V. Siva Kumar, B.S. Murty, V.R.K. Murthy, *J. Phys. D.* **2007**, *40*, 7565. DOI: [10.1088/0022-3727/40/23/049](https://doi.org/10.1088/0022-3727/40/23/049)
20. W.H. Robinson, A. Edger, *IEEE Trans. Sonic and Ultrasonics*, **1974**, *21*, 98.
DOI: [10.1109/T-SU.1974.29798](https://doi.org/10.1109/T-SU.1974.29798)
21. Y. Hiruma, H. Nagata, T. Takenaka, *J. Appl. Phys.* **2009**, *105*, 084112.
DOI: [10.1063/1.3115409](https://doi.org/10.1063/1.3115409)
22. J. Suchanicz, J.-P. Mercurio, P. Marchet, T.V. Kruzina, *Phys. Status Solidi. B* **2001**, *225*, 459.
DOI: [10.1002/1521-3951\(200106\)225:2.459](https://doi.org/10.1002/1521-3951(200106)225:2.459)
23. V. Dorcet, P. Marchet, G. Trolliard, *J. Eur. Ceram. Soc.* **2007**, *27*, 4371.
DOI: [10.1016/j.jeurceramsoc.2007.02.173](https://doi.org/10.1016/j.jeurceramsoc.2007.02.173)
24. I.P. Pronin, P.P. Syrnikov, V.A. Isupov, V.M. Egorov, N.V. Zaitseva, *Ferroelectrics* **1985**, *25*, 395.
DOI: [10.1080/00150198008207029](https://doi.org/10.1080/00150198008207029)
25. I.P. Pronin, P.P. Syrnikov, V.A. Isupov, G.A. Smolenskii, Pis'mav Zh Tekh Fiz. **1982**, *8*, 1309. (*Sov. Technol. Phys. Lett.* **1982**, *8*, 563.)
26. W. Ge, C. Luo, Q. Zhang, C.P. Devreugd, Y. Ren, J. Li, H. Luo, D. Viehland, *J. Appl. Phys.* **2012**, *111*, 093508.
DOI: [10.1063/1.4709619](https://doi.org/10.1063/1.4709619)
27. Cheuk Wai Tai, W.Z. Siu Hong Choy, Helen L. W. Chan, *J. Am. Ceram. Soc.* **2008**, *91*, 3335.
DOI: [10.1111/j.1551-2916.2008.02592.x](https://doi.org/10.1111/j.1551-2916.2008.02592.x)
28. H. Xu, *Ferroelectric Materials and Their Applications*, North Holland, New York, **1991**.
29. J. J. Suchanicz, *J. Mater. Sci.* **2002**, *37*, 489.
DOI: [10.1023/A:1013705204937](https://doi.org/10.1023/A:1013705204937)

30. T. Oh, *Jpn. J. Appl. Phys.*, **2006**, *45*, 5138.
DOI: [10.1143/JJAP.45.5138](https://doi.org/10.1143/JJAP.45.5138)
31. Y.N. Wang, Y.N. Huang, H.M. Shen, Z.F. Zhang, *J. Phys. III* 1996, *6*, C8-505.
DOI: [10.1051/jp4:19968110](https://doi.org/10.1051/jp4:19968110)
32. V.S. Postnikov, V.S. Pavlov, S.K. Turkov, *J. Phys. Chem. Solids.* **1996**, *31*, 1785.
DOI: [10.1016/0022-3697\(70\)90168-X](https://doi.org/10.1016/0022-3697(70)90168-X)
33. X.M. Xie, T.G. Chen, Z.L. Wu, *Phys. Rev. B.* **1989**, *40*, 4549.
DOI: [10.1103/PhysRevB.40.4549](https://doi.org/10.1103/PhysRevB.40.4549)
34. N. Nowick B.S. Berry, "Anelastic Relaxation in Crystalline Solids," New York and London: Academic Press, **1972**.
35. W. Yening, S. Wenyuan, C. Xiaohua, S. Huimin, L. Baosheng, *Phys. Stat. Solidi A* **1987**, *102*, 279.
DOI: [10.1002/pssa.2211020128](https://doi.org/10.1002/pssa.2211020128)
36. W. L. Warren, B. A. Tuttle, D. Dimos, *Appl. Phys. Lett.* **1995**, *67*, 1426.
DOI: [10.1063/1.114515](https://doi.org/10.1063/1.114515)
37. P. R. Graves, G. Hua, S. Myhra, and J. G. Thompson, *J. Solid State Chem.* **1991**, *112*.
DOI: [10.1006/jssc.1995.1017](https://doi.org/10.1006/jssc.1995.1017)

Advanced Materials Letters

Publish your article in this journal

[ADVANCED MATERIALS Letters](#) is an international journal published quarterly. The journal is intended to provide top-quality peer-reviewed research papers in the fascinating field of materials science particularly in the area of structure, synthesis and processing, characterization, advanced-state properties, and applications of materials. All articles are indexed on various databases including [DOAJ](#) and are available for download for free. The manuscript management system is completely electronic and has fast and fair peer-review process. The journal includes review articles, research articles, notes, letter to editor and short communications.

